Chapter 5

The Nature of Boxy/Peanut-Shaped Bulges in Spiral Galaxies

Abstract

We present a systematic observational study of the relationship between bars and boxy/peanut-shaped (B/PS) bulges in spiral galaxies. We first review and discuss proposed mechanisms for the formation of B/PS bulges, focussing on accretion and bar-buckling scenarios. Using new methods relying on the kinematics of edge-on disks, we look for bars in a large sample of edge-on spiral galaxies with B/PS bulges and in a smaller control sample of edge-on spirals with more spheroidal bulges. We present position-velocity diagrams of the ionised gas obtained from optical long-slit spectroscopy. We show that almost all B/PS bulges are due to a thick bar viewed edge-on, while only a few extreme cases are likely due to the accretion of external material. This strongly supports the bar-buckling mechanism for the formation of B/PS bulges. None of the galaxies in the control sample shows evidence for a bar, which suggests conversely that bars are generally B/PS.

We consider the effects of dust in the disk of the galaxies, but conclude that it does not significantly affect our results. Unusual emission line ratios correlating with kinematical structures are observed in many objects, and we argue that this is consistent with the presence of strong bars in the disk of the galaxies. More work is required to determine the orientation of the bars in B/PS bulges.

The reliable identification of bars in edge-on spiral galaxies opens up for the first time the possibility of studying observationally the vertical structure of bars.

5.1 Introduction

Many spiral galaxies display boxy or peanut-shaped bulges when viewed edge-on. Statistical studies of the incidence of these objects have not used objective criteria to quantify the boxiness of the bulges. They are therefore hard to compare and yield moderately different results. Nevertheless, it seems clear that at least 20–30% of edge-on spirals possess a boxy/peanut-shaped (B/PS) bulge (see Jarvis 1986; Shaw 1987; de Souza & dos Anjos 1987). Spiral galaxies with B/PS bulges are therefore a significant class of objects.

The fact that the boxy/peanut shape is seen only in edge-on spirals indicates that the shape is related to the vertical distribution of the light. B/PS bulges have excess light above the plane at large galactocentric radii, compared to the usual $R^{1/4}$ law for the light distribution of spheroids (see Shaw 1993). Their three-dimensional light distribution must be even more extreme than the projected surface brightness (see, e.g., Binney & Petrou 1985 for axisymmetric models). In addition, B/PS bulges appear to rotate cylindrically, i.e. their rotation is independent of the height above the plane (e.g. Kormendy & Illingworth 1982; Rowley 1986).

Several models have been proposed to explain the structure of these bulges (e.g. Combes & Sanders 1981; May, van Albada, & Norman 1985; Binney & Petrou 1985). However, despite their prevalence and interesting structural and dynamical properties, they remain poorly studied observationally, probably because the edge-on projection makes the interpretation of observational data difficult.

In this chapter, we present new kinematical data for a large sample of spiral galaxies with a B/PS bulge. Our goal is to determine their three-dimensional structure and to identify their likely formation mechanism. We use our data to argue that B/PS bulges are simply bars viewed edge-on.

In § 5.2, we discuss the two main scenarios proposed for the formation of B/PS bulges – accretion of satellite galaxies and buckling of a bar. In § 5.3, we describe ways to discriminate between the two formation scenarios using kinematical data. The observations are presented in § 5.4 and the results discussed in § 5.5. We conclude in § 5.6.

5.2 Formation Mechanisms

5.2.1 Accretion

In early studies, the accretion of external material such as satellite galaxies was the favoured mechanism to explain the formation of B/PS bulges in spiral galaxies.

Binney & Petrou (1985) and Rowley (1986, 1988) showed that it is possible to construct axisymmetric cylindrically rotating B/PS bulges from relatively simple distribution functions. Binney & Petrou adopted a distribution function with a third integral of motion, in addition to the energy E and angular momentum along the symmetry axis L_z. This integral favoured orbits reaching a particular height above the plane. Rowley adopted a two-integral distribution function, with a truncation depending on both E and L_z. Both authors argued that the required distribution function could form naturally through the accretion of material onto a host spiral galaxy. Binney & Petrou (1985) additionally argued that, for the accreted material to form a B/PS bulge, the velocity dispersion of the accreted satellite must be much lower than the orbital speed, and the decay timescale must be much longer that the orbital time. This ensures that the accreted material stays clustered in phase space.

Accretion scenarios face several problems. At one extreme, one can consider the accretion of several small satellite galaxies. However, only a narrow range of orbital energy and angular momentum can lead to the formation of a B/PS bulge (Binney & Petrou 1985), so it is improbable that many satellite galaxies would all share these properties. Remaining satellites should then be present but they are not observed (Shaw 1987). The accretion of a single large companion is also ruled out by the large velocity dispersion and small decay timescale involved (Binney & Petrou 1985). Similarly, the merger of two spiral galaxies of similar sizes (or of a spiral and a small elliptical) seems an unlikely route to form B/PS bulges. This would require a fairly precise alignment of the spin and orbital angular momenta of the two galaxies. We recall that about a third of spiral galaxy bulges must be formed in this way (e.g. Shaw 1987).

From the arguments presented above, it seems that the accretion of a small number of moderate-sized satellites is the only accretion scenario which may lead to the formation of B/PS bulges. In favour of accretion is the fact that the best examples of B/PS bulges are found in small groups (e.g. NGC 128 and ESO 597-G 036), although we note that spirals with a B/PS bulge are not found preferentially in clusters (Shaw 1987). In addition, the possibly related X-shaped galaxies can form through the accretion of a satellite (e.g. Whitmore & Bell 1988; Hernquist & Quinn 1989). On the other hand, no evidence of accretion (arcs, shells, filaments, etc.) were detected by Shaw (1993) near spirals with a B/PS bulge, which argues against any kind of accretion. We are thus led to the conclusion that, while accretion of external material may play a role in the formation of some B/PS bulges, it is unlikely to be the primary formation mechanism.

5.2.2 Bar-Buckling

Bars can form naturally in N-body simulations of rotationally supported stellar disks (e.g. Sellwood 1981; Athanassoula & Sellwood 1986), due to global bisymmetric instabilities (e.g. Kalnajs 1971, 1977). Based on 3D N-body simulations, Combes & Sanders (1981) were the first to suggest that B/PS bulges could arise from the thickening of bars in the disks of spiral galaxies. Their results were confirmed and their suggestion supported by many later studies (see, e.g., Combes et al. 1990; Raha et al. 1991). Essentially, soon after a bar develops, it buckles, and settles with an increased thickness and vertical velocity dispersion, appearing boxy-shaped when seen end-on and peanut-shaped when seen side-on. The B/PS bulges thus formed are cylindrically rotating, as required.

Toomre (1966) first considered the buckling of disks, using idealised models, and found that if the vertical velocity dispersion in a disk is less than about a third of the velocity dispersion in the plane, the disk will be unstable to buckling modes (fire-hose or buckling instability; see also Fridman & Polyachenko 1984; Araki 1985). Bar formation in a disk makes the orbits within the bar more eccentric, without significantly affecting their perpendicular motions, thereby providing a natural mechanism for the bar to buckle. Resonances between the rotation of the bar and the vertical oscillations of the stars can also make the disk vertically unstable (see Pfenniger 1984; Combes et al. 1990; Pfenniger & Friedli 1991). The final shape of the bar is probably due to orbit trapping around the 2:2:1 periodic orbit family (see, e.g., Pfenniger & Friedli 1991).

Bar-buckling is the currently favoured mechanism for the formation of B/PS bulges. The fraction of edge-on spiral galaxies possessing a B/PS bulge is similar to the fraction of strongly barred spirals in face-on systems ($\approx 30\%$; e.g. Sellwood & Wilkinson 1993). In addition, bar-buckling provides a natural way to form B/PS bulges in isolated spiral galaxies, which accretion scenarios cannot do. We recall that spiral galaxies with a B/PS bulge are not found preferentially in clusters (Shaw 1987). We also note that, in a few cases, a bar can be directly associated with a B/PS bulge from morphological arguments (see, e.g., Bettoni & Galletta 1994 for NGC 4442).

The main observational problem faced by the bar-buckling mechanism is that B/PS bulges appear to be shorter (relative to the disk diameter) than real bars or strong bars formed in N-body simulations. However, this might simply be due to projection (a given surface brightness level is reached at a smaller radius in a more face-on disk) and no proper statistics have yet been compiled. The long term secular evolution of bars is also poorly understood. For example, it is known that bars can transfer angular momentum to a spheroidal component very efficiently (e.g. Sellwood 1980; Weinberg 1985). However, Debattista & Sellwood (1998) showed that, while the bar can be slowed down, it continues to grow and

the boxy/peanut shape is preserved. It is less clear what happens if a bar is strongly perturbed. Norman, Sellwood, & Hasan (1996) also showed that if a bar is destroyed through the growth of a central mass concentration (e.g. Friedli & Benz 1993; Hasan & Norman 1990), the boxy/peanut shape is also destroyed.

The merits of the bar-buckling mechanism outweigh these potential problems, and the bar-buckling scenario remains largely unchallenged at the moment, despite very little direct observational confirmation (see, however, Kuijken & Merrifield 1995). The main aim of this chapter is to directly test this hypothesis by looking for bars in a large sample of spiral galaxies with a B/PS bulge.

Although it is not part of our program, the Milky Way is the first example of such a galaxy. The Galactic bulge is boxy-shaped (Weiland et al. 1994) and it is now well established that it is bar-like (e.g. Binney et al. 1991; Paczyński et al. 1994; see Kuijken 1996 for a brief review of the subject).

We note that "hybrid" scenarios have been proposed to explain the formation of B/PS bulges. An interaction or merger can excite (or accelerate) the development of a bar in a disk which is stable (or quasi-stable) against bar formation (e.g. Noguchi 1987; Gerin, Combes, & Athanassoula 1990; Miwa & Noguchi 1998). Bars formed this way are free to evolve to a boxy/peanut shape in the manner described above (see, e.g., Mihos et al. 1995), and the bulges thus formed owe as much to interaction as they do to the bar-buckling instability. However, the *shape* of the bulges is due to the buckling of the bars and interaction is merely a way to start the process of bar formation. In that sense, hybrid scenarios for the formation of B/PS bulges are really bar-buckling scenarios, and the possible accretion of material is unrelated to the shape of the bulges.

5.3 Observational Diagnostics

The main purpose of the observations presented in this chapter is to search for bars in the disks of spiral galaxies possessing a B/PS bulge. There is no straightforward photometric method to identify a bar in an edge-on spiral galaxy. The presence of a plateau in the major-axis light profile of the disk has been invoked as an indicator of the presence of a bar (e.g. de Carvalho & da Costa 1987; Hamabe & Wakamatsu 1989). However, axisymmetric features (e.g. a lens) can be mistaken for a bar and end-on bars may remain undetected. Kuijken & Merrifield (1995) were the first to demonstrate that bars could be identified kinematically in external edge-on spiral galaxies. They showed that the periodic orbits in a barred galaxy model produce characteristic double-peaked line-of-sight velocity distributions when viewed edge-on (see also Merrifield 1996). This gives long-slit spectra a spectacular "figure-of-eight" (or X-shaped) appearance, which they were able to observe in two systems with a B/PS bulge, namely NGC 5746

and NGC 5965 (see Fig. 5.1 for examples). Their approach is analogous to that used in the Galaxy with longitude-velocity diagrams (e.g. Peters 1975; Mulder & Liem 1986; Binney et al. 1991).

In Chapter 3, we refined the dynamical theory of Kuijken & Merrifield (1995). We used periodic orbit families in a barred galaxy model as building blocks to model the structure and kinematics of real galaxies. We showed that the global structure of a position-velocity diagram[1] (PVD) taken along the major axis of an edge-on system is a reliable bar diagnostic, particularly the presence of gaps between the signatures of the different periodic orbit families. In Chapter 4, we developed similar bar diagnostics using hydrodynamical simulations of the gaseous component alone. We showed that, when a nuclear spiral is present (corresponding to the existence of x_2 orbits, or equivalently of an inner Lindblad resonance), the presence of a gap in the PVD between the signature of the nuclear spiral and that of the outer parts of the disk reliably indicates the presence of a bar. If no nuclear spiral is present, one must rely on indirect evidence to argue for the presence of a bar. These gaps are a direct consequence of the shocks which develop in relatively strong bars. These shocks drive an inflow of gas toward the center of the galaxies and deplete the main and outer bar regions (see, e.g., Athanassoula 1992). The simulations in Chapter 4 can be directly compared with the emission line spectra presented here, and will form the basis of our argument.

These models can also be used to determine the viewing angle with respect to a bar, as the features present in the PVDs change with the orientation of the line-of-sight (see Ch. 3 and 4). In particular, when a bar is seen end-on, the signature of the flow associated with the x_1 orbits (the main bar region, elongated parallel to the bar) reaches very high radial velocities, while the signature of the flow associated with the x_2 orbits (the nuclear spiral, elongated perpendicular to the bar) shows only relatively low velocities. The opposite is true when a bar is seen side-on. In addition, the presence or absence of a nuclear spiral signature can somewhat constrain the mass distribution and bar pattern speed of an observed galaxy.

We have not developed specific observational criteria to identify past or current accretion of material in the observed galaxies. As discussed in § 5.2.1, accretion will occur through interaction or merger events. We will take as the signature of such events, and of possible accretion, the presence of irregularities in the observed PVDs, in particular strong asymmetries about the center of an object (see Fig. 5.1 for examples).

[1]Position-velocity diagrams (PVDs) show the projected density of material as a function of line-of-sight velocity and projected position.

5.4 Observations

5.4.1 The Sample

Our sample of galaxies consists of 30 edge-on spirals selected from the catalogues of Jarvis (1986), Shaw (1987), and de Souza & dos Anjos (1987) (spiral galaxies with a B/PS bulge), and from the catalogue of Karachentsev, Karachentseva, & Parnovsky (1993) (spiral galaxies with extreme axial ratios; see also Karachentsev et al. 1993). In order to have enough spatial resolution for the long-slit spectroscopy, but still be able to image the galaxies relatively quickly with a small-field near-infrared camera, we have selected objects with bulges larger than about 0.′6 in diameter and disks smaller than about 7.′0 (at the 25 B mag arcsec^{-2} level). All objects are accessible from the south ($\delta \leq 15°$). Two-thirds (21/30) of the galaxies either have probable companions or are part of a group or cluster. A few of these may be chance alignments, but it is fair to say that we are not biased either against or in favour of galaxies in a dense environment. We should therefore be able to estimate reliably the relative importance of accretion in the formation of B/PS bulges.

Of the sample galaxies described above, 80% (24/30) have a boxy or peanut-shaped bulge, while 20% (6/30) have a bulge of spheroidal morphology. Of the former group, 17 galaxies have emission lines extending far enough in the disk that we can apply the diagnostics developed in Chapters 3 and 4 using the ionised gas; all galaxies in the control group fulfill this condition. In this chapter, we will thus concentrate on a main sample of 17 edge-on spiral galaxies with B/PS bulges and on a "control" sample of 6 edge-on spiral galaxies with more spheroidal bulges. The galaxies in each sample are listed in Tables 5.1 and 5.2, along with information on their properties and environment. The galaxies with no or confined emission are listed in Table 5.3. We note that the galaxy type listed is not very reliable, as it is difficult to classify edge-on spirals.

Other than the catalogue of Karachentsev et al. (1993), we are not aware of any general catalogue of edge-on spiral galaxies. It is thus difficult to construct a large and varied control sample including edge-on spiral galaxies with large bulges (the Karachentsev et al. 1993 catalogue is restricted to galaxies with a major to minor axis ratio $a/b \geq 7$). Such a catalogue would be very useful.

5.4.2 Observations and Data Reduction

Our spectroscopic data were acquired over a total of 39 nights between December 1995 and May 1997, using the Double Beam Spectrograph on the 2.3 m telescope at Siding Spring Observatory. A 1752 $\times$ 532 pixels SITE ST-D06A

Table 5.1: Main Sample

Galaxy	Type	Bulge	Environment	Structure	Notes
NGC 128	S0 pec	Peanut	In group	Bar[a]	···
ESO 151- G 004	$S0^0$	Peanut	In group	Bar	···
NGC 1886	Sab	Boxy	Isolated	Bar	···
NGC 2788A	Sb	Peanut	In cluster	Bar	Dusty
IC 2531	Sb	Peanut	In cluster	Bar[b]	Dusty
NGC 3390	Sb	Boxy	Companions?	Accretion	···
NGC 4469	SB(s)0/a?	Peanut	Companions	Axisymmetric	···
NGC 4710	$SA(r)0^+$	Boxy	Isolated	Bar	···
PGC 44931	Sbc	Peanut	Isolated	Bar	···
ESO 443- G 042	Sb	Peanut	Companions?	Bar	Dusty
NGC 5746	SAB(rs)b?	Peanut	Isolated	Bar	···
NGC 6722	Sb	Peanut	Isolated	Bar	···
NGC 6771	$SB(r)0^+$?	Peanut	In group	Bar	···
IC 4937	Sb	Peanut	In cluster	Bar	Dusty
ESO 597- G 036	$S0^0$ pec	Peanut	In group	Accretion	Dusty
IC 5096	Sb	Boxy	Companions?	Bar	···
ESO 240- G 011	Sb	Boxy	In group	Bar	···

[a]Emsellem & Arsenault (1997)
[b]Bureau & Freeman (1997)

Table 5.2: Control Sample

Galaxy	Type	Bulge	Environment	Structure	Notes
NGC 1032	S0/a	Spheroidal	Companions	Axisymmetric	Dusty
NGC 3957	$SA0^+$	Spheroidal	In cluster	Axisymmetric	···
NGC 4703	Sb	Spheroidal	Isolated	Axisymmetric	Dusty
NGC 5084	S0	Spheroidal	In cluster	Accretion	···
NGC 7123	Sa	Spheroidal	Isolated	Accretion	Dusty
IC 5176	SAB(s)bc?	Spheroidal	Companions?	Axisymmetric	···

Table 5.3: Galaxies with No or Confined Emission

Galaxy	Type	Bulge	Environment	Notes
NGC 1381	SA0	Boxy	In cluster	···
NGC 1596	SA0	Boxy	In group	···
NGC 2310	S0	Boxy	Isolated	···
ESO 311- G 012	S0/a?	Boxy	Isolated	···
NGC 3203	$SA(r)0^+$?	Boxy	In group	···
IC 4767	S pec	Peanut	In cluster	···
ESO 185- G 053	SB pec	Peanut	In cluster	···

thinned CCD was used. The observations discussed in this chapter were obtained with the red arm of the spectrograph centered on the Hα λ6563 emission line. All galaxies were observed using a $1\farcs8 \times 400''$ slit aligned with the major axis. For objects with a strong dust lane, the slit was positioned just above it. The spectral resolution is about 1.1 Å FWHM (0.55 Å pixel^{-1}) and the spatial scale is $0\farcs9$ pixel^{-1}. These data can be directly compared with the PVDs obtained from the hydrodynamical simulations of Chapter 4. When no emission line was detected in an object, the red arm of the spectrograph was moved to the Ca II absorption line triplet. The blue arm was always centered on the Mg b absorption feature. These data will form the core of a future paper discussing the stellar kinematics of the sample galaxies (including the galaxies in Table 5.3). Total exposure times on both arms ranged from 12000 to 21000 s per object.

The spectra were reduced using standard procedures in IRAF. The data were first bias-subtracted, using both the vertical and horizontal overscan regions, and then using bias frames. If necessary, the data were also dark-subtracted. The spectra were then flatfielded using flattened continuum lamp exposures, and wavelength-calibrated using bracketing arc lamp exposures for each image. The data were then rebinned to a logarithmic wavelength (linear velocity) scale corresponding to 25 km s^{-1} pixel^{-1}. The spectra were then corrected for vignetting along the slit using sky exposures. All exposures of a given object were then registered and offset along the spatial axis, corrected to a heliocentric rest frame, and combined. The resulting spectra were then sky-subtracted using source-free regions of the slit on each side of the objects. The sky subtraction was less than perfect in some cases because of difficulties in obtaining a uniform focus of the spectrograph along the entire length of the CCD. This was particularly troublesome for objects like IC 2531 and NGC 5746 which extend over almost the entire length of the slit (see, e.g., Fig. 5.3a). In order to isolate the emission lines, the continuum emission of the objects was then subtracted using a low-order fit to the data. The resulting spectra constitute the basis of our discussion in the next section.

We note that in regions with bright continuum emission, like the centers of some galaxies, the continuum subtraction can leave relatively high shot noise in the data, which should not be confused with line emission in the grayscale plots of Figures 5.1–5.3. This is the case, for example, in the spectra of ESO 240- G 011, NGC 1032, and NGC 4703 (Figs. 5.1 and 5.2). The effect is perhaps best seen when a bright star is subtracted, such as seen in the spectra of NGC 2788A or NGC 1032 (see, again, Figs. 5.1 and 5.2).

We have not extracted rotation curves from our data. This is because we require the entire two-dimensional spectrum, or PVD, to identify the signature of a bar in an edge-on galaxy (see Ch. 3 and 4). Evidence of interaction and of

possible accretion are also more easily seen in the two-dimensional spectra. We present spectra of the [N II] λ6584 emission line rather than the Hα line because it is not affected by underlying stellar absorption.

5.4.3 Results

We present here our emission line spectra for all the sample galaxies which have extended emission. The PVDs of the galaxies in the main sample are shown in Figure 5.1 and those of the control sample are shown in Figure 5.2. In order to illustrate the range of galaxy types and bulge morphologies in the sample, and to allow connections to be made between bulge morphologies and kinematical features in the disks, each PVD is accompanied by a registered image of the corresponding galaxy (Digitized Sky Survey) on the same spatial scale. We will discuss here the trends observed across the data set.

The most important trend, and the main result of this chapter, is that most of the galaxies in the main sample show a clear bar signature in their PVD (as described in § 5.3). Of the 17 galaxies in the main sample of spirals with a B/PS bulge and extended emission lines, we conclude that 14 galaxies are barred[2]. In these objects, the PVD clearly shows a strong and steep inner component, associated with a nuclear spiral (an x_2-like flow), and a slowly-rising almost solid-body component, associated with the outer parts of the disk, and joining the flat section of the rotation curve at large distances. Those two components are separated by a gap caused by the absence of gaseous material with an x_1-like behaviour in the barred region. The best examples of this type of bar signature, discussed in Chapters 3 and 4, are seen in the PVD of earlier-type objects, like NGC 2788A, NGC 5746, and IC 5096. However, the signature is still clearly visible in the PVD of galaxies as late as ESO 240- G 011 (see Fig. 5.1).

In the main sample, only one galaxy, NGC 4469, may be axisymmetric, with no evidence of either a bar or interaction. Two galaxies, NGC 3390 and ESO 597-G 036, have disturbed asymmetric PVDs, which we ascribe to recent interactions (obvious in the case of ESO 597- G 036). These interactions may have led to the accretion of external material. The results for the whole main sample are summarised in Table 5.1.

Another significant result of this study is that no galaxy in the control sample shows evidence for a bar. Four of the six galaxies appear to be axisymmetric, without evidence for either a bar or interaction, and two galaxies (NGC 5084 and NGC 7123) have a disturbed PVD, indicating that they underwent an interaction

[2]The PVDs of NGC 128 and IC 2531 do not display a bar signature, but Emsellem & Arsenault (1997) and Bureau & Freeman (1997) showed, using other data, that each galaxy harbours a bar.

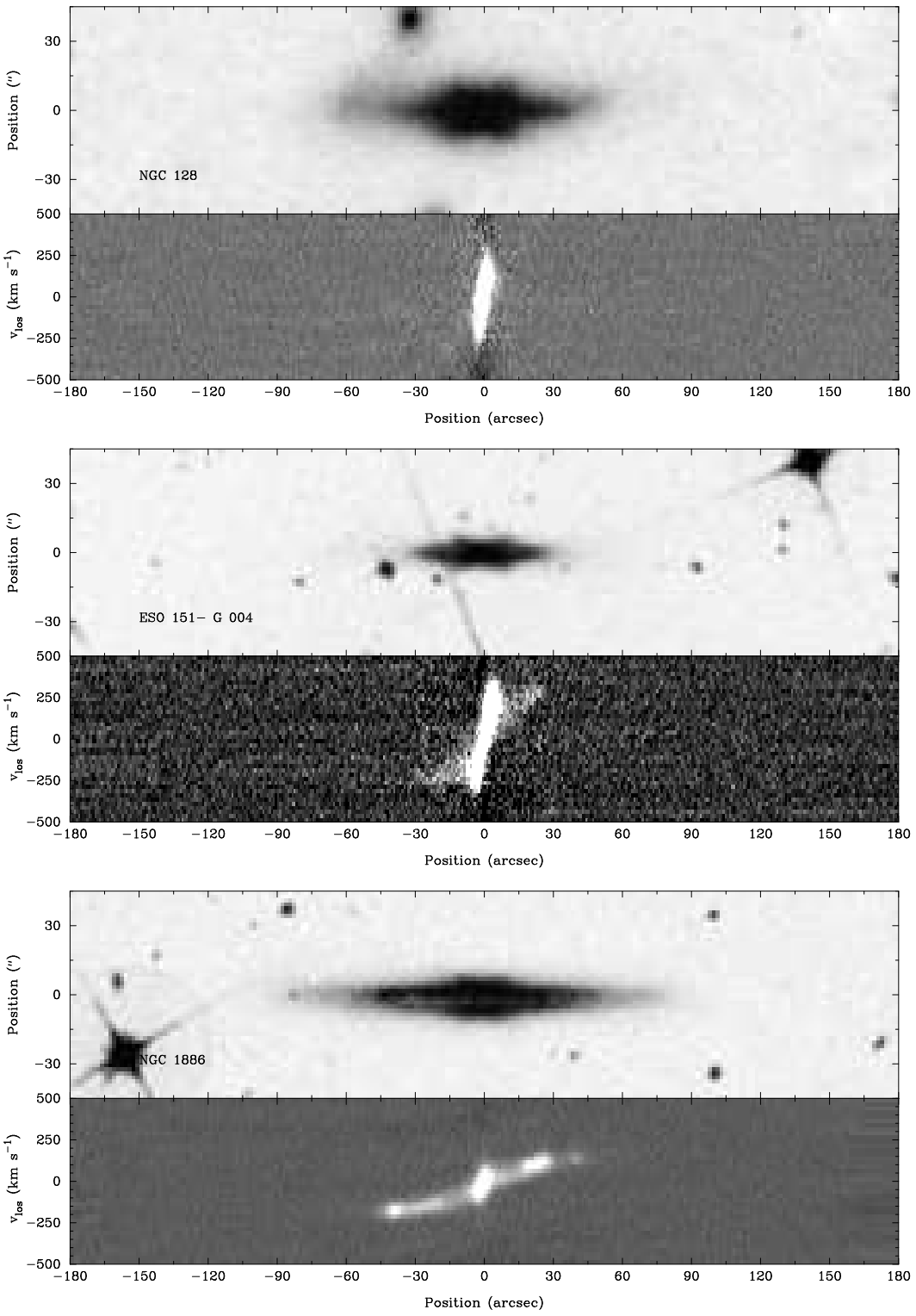

Figure 5.1: Structure and kinematics of the galaxies in the main sample of spirals with boxy/peanut-shaped bulges. Each plot corresponds to a galaxy. For each plot, the top panel shows a blue image of the galaxy (Digitized Sky Survey), which is identified in the bottom-left corner. The bottom panel shows the ionised gas ([N II] λ6584) position-velocity diagram (PVD) of the galaxy along its major axis, registered with the image above it. The galaxies are ordered as in Table 5.1.

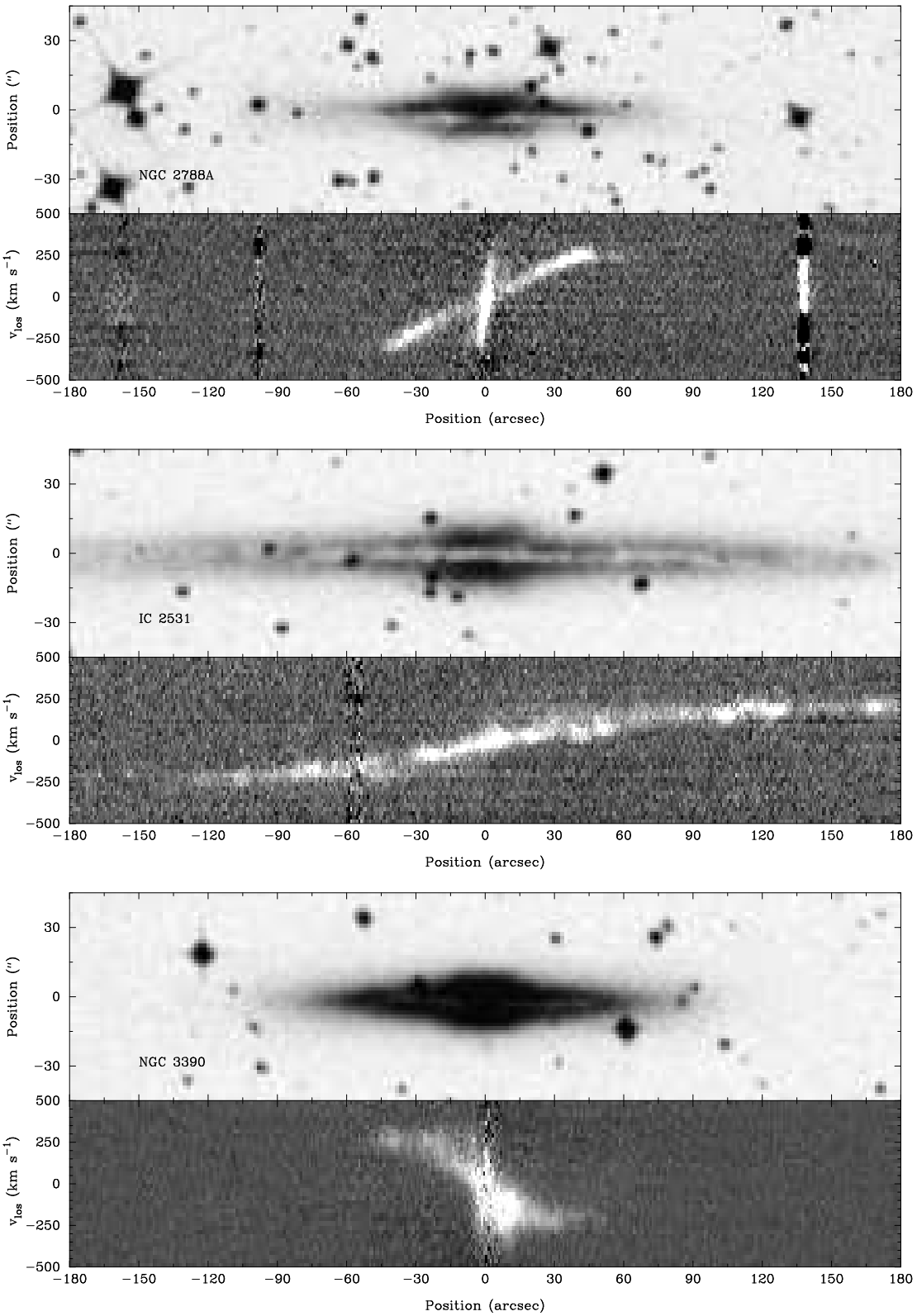

Figure 5.1: *Continued.*

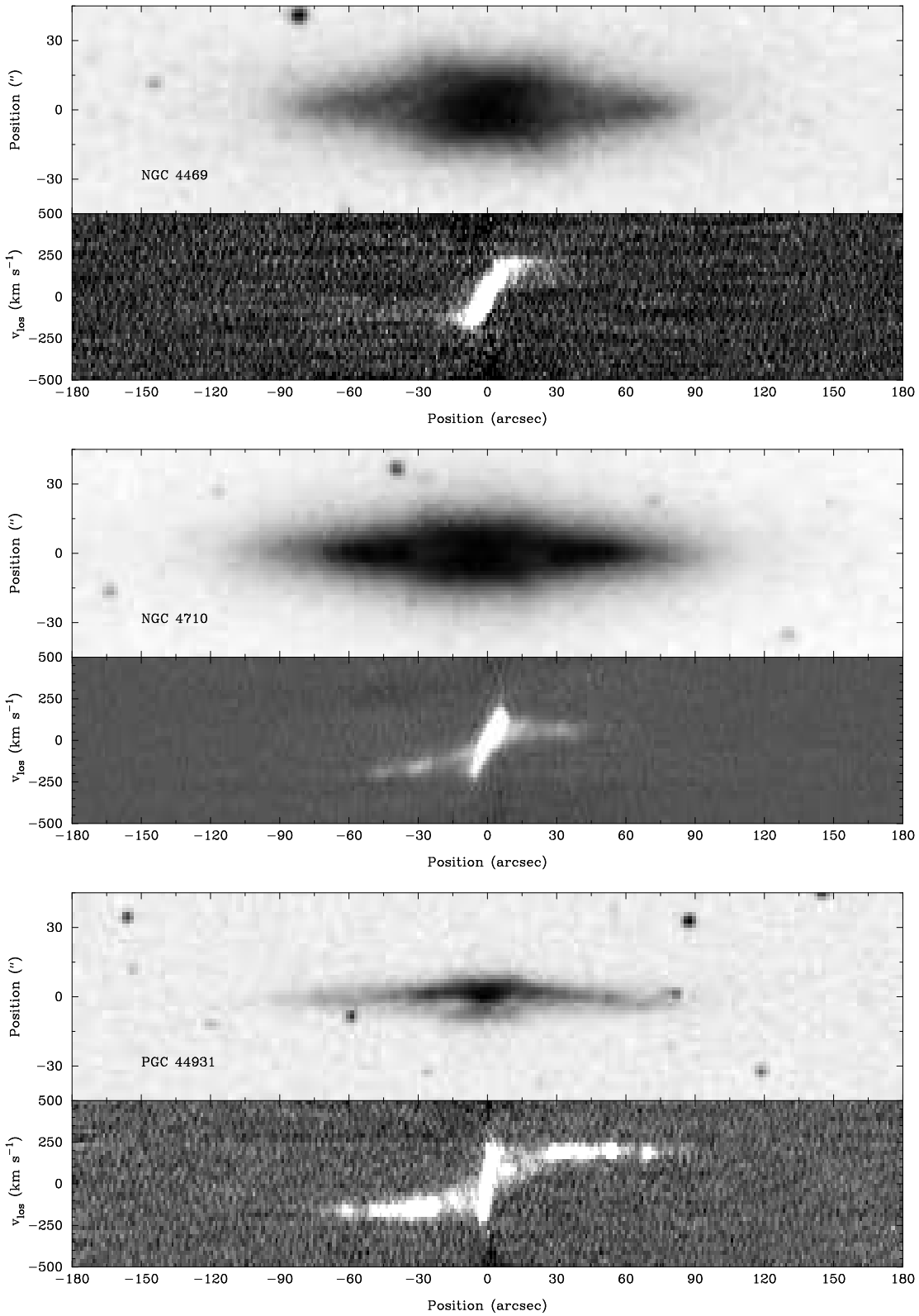

Figure 5.1: *Continued.*

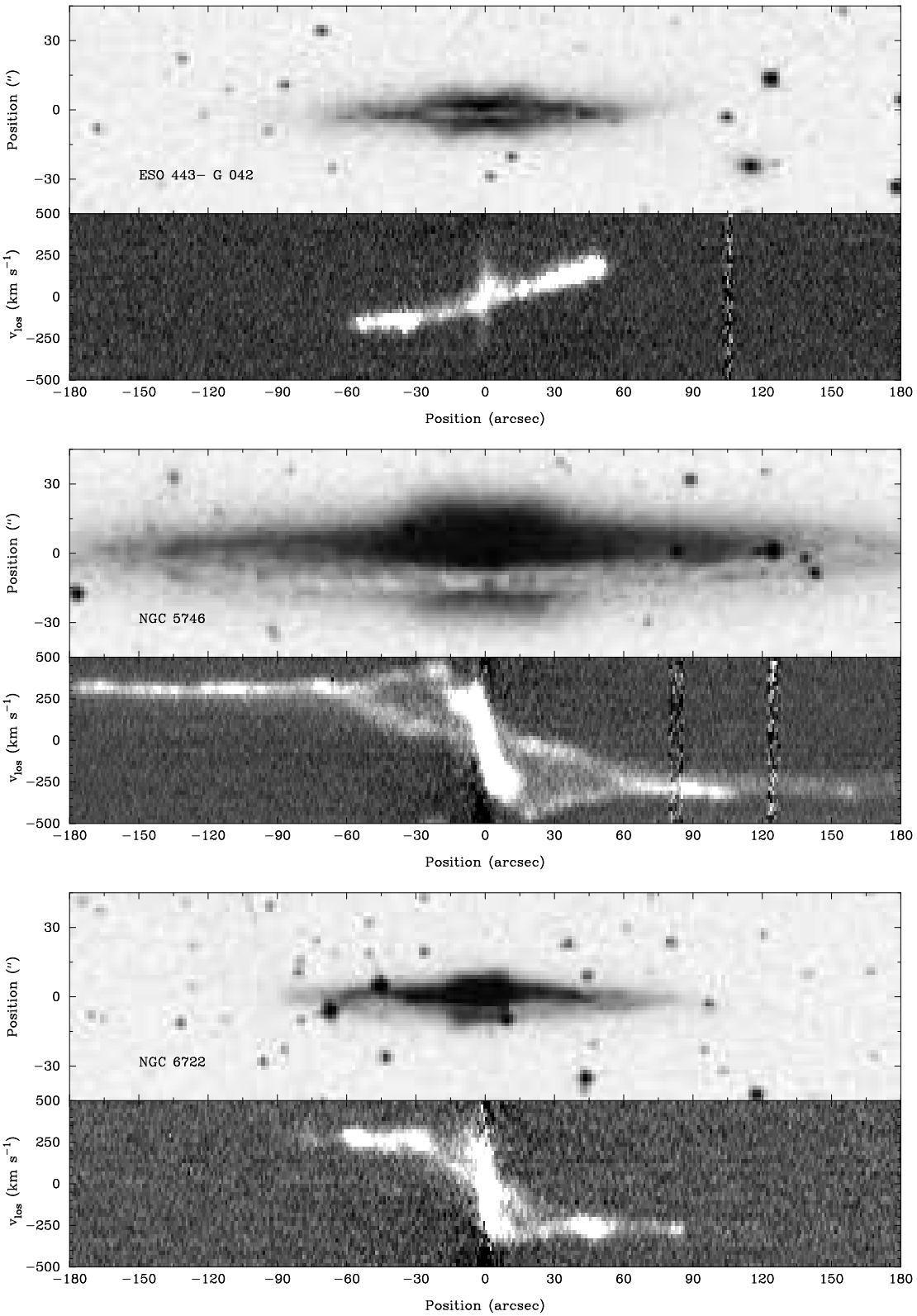

Figure 5.1: *Continued.*

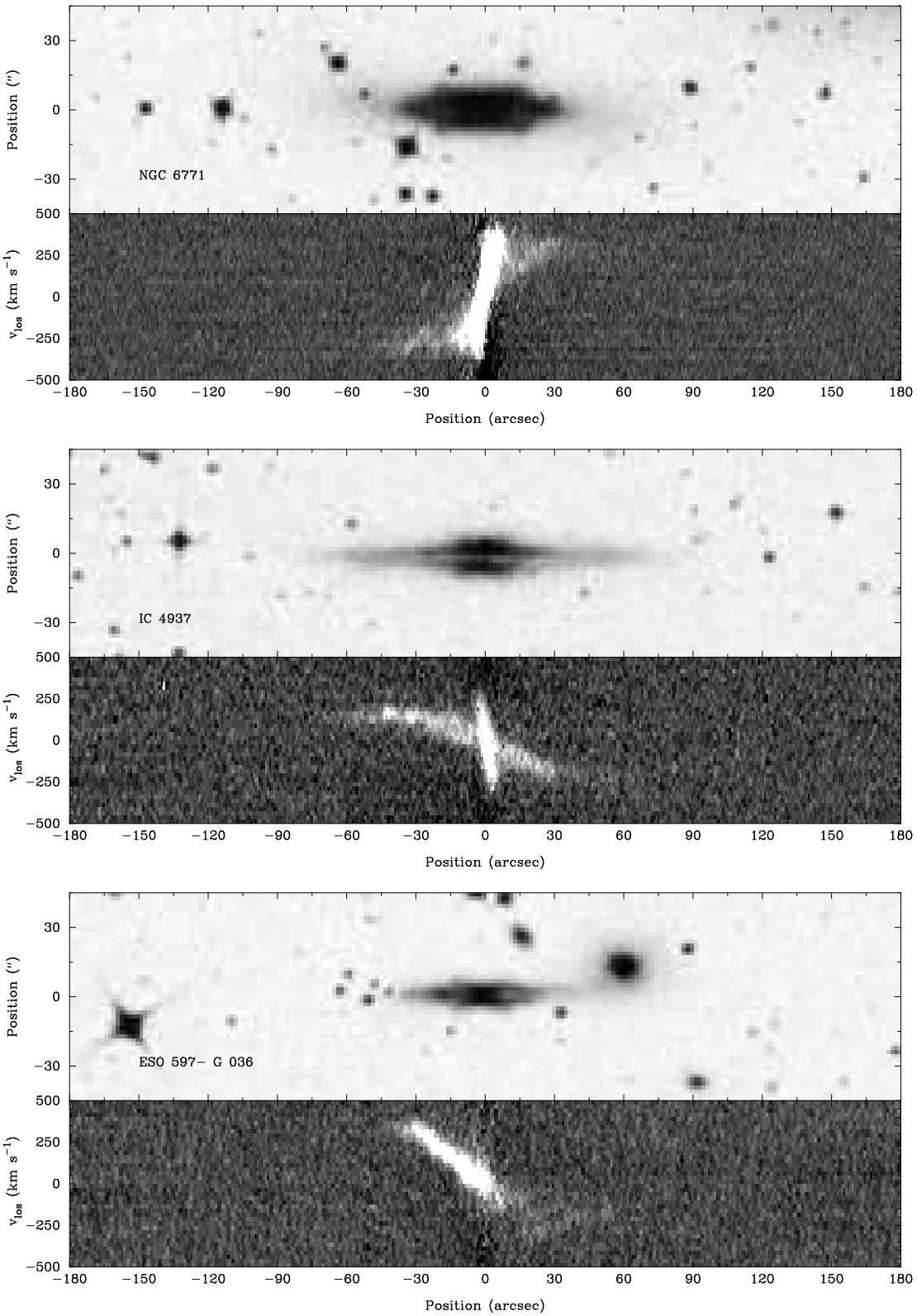

Figure 5.1: *Continued.*

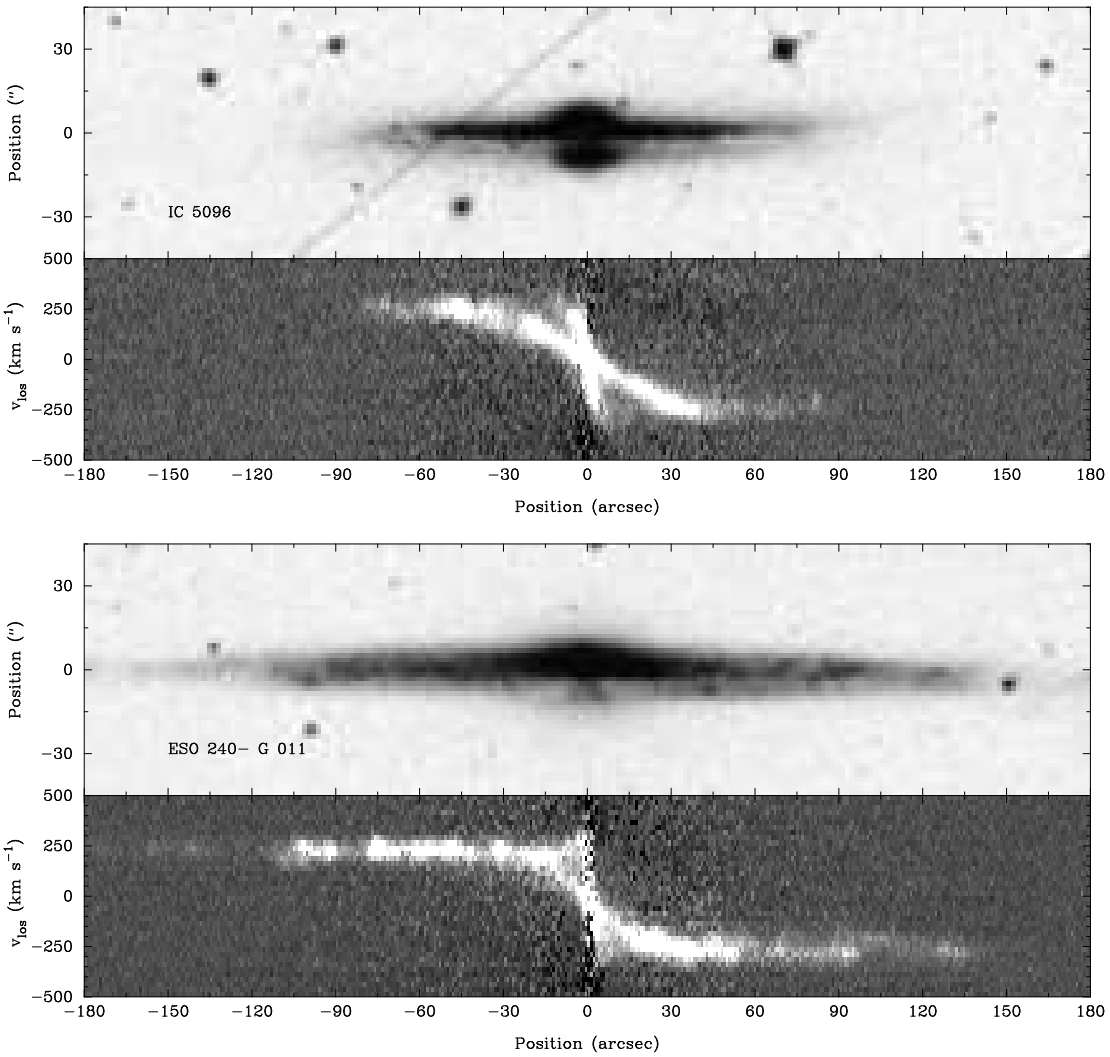

Figure 5.1: *Continued.*

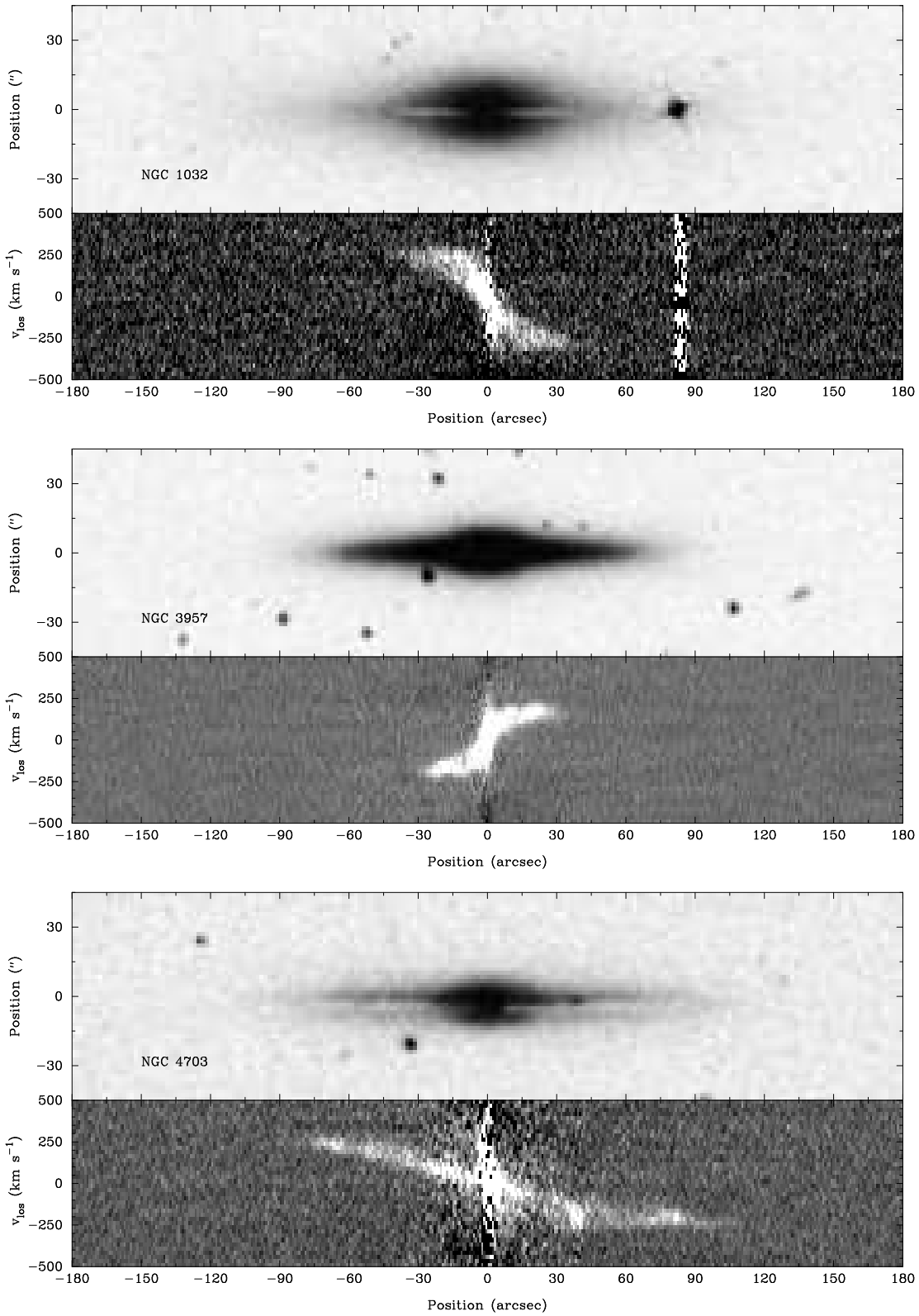

Figure 5.2: Same as Figure 5.1 but for the control sample of spirals with spheroidal bulges. The galaxies are ordered as in Table 5.2.

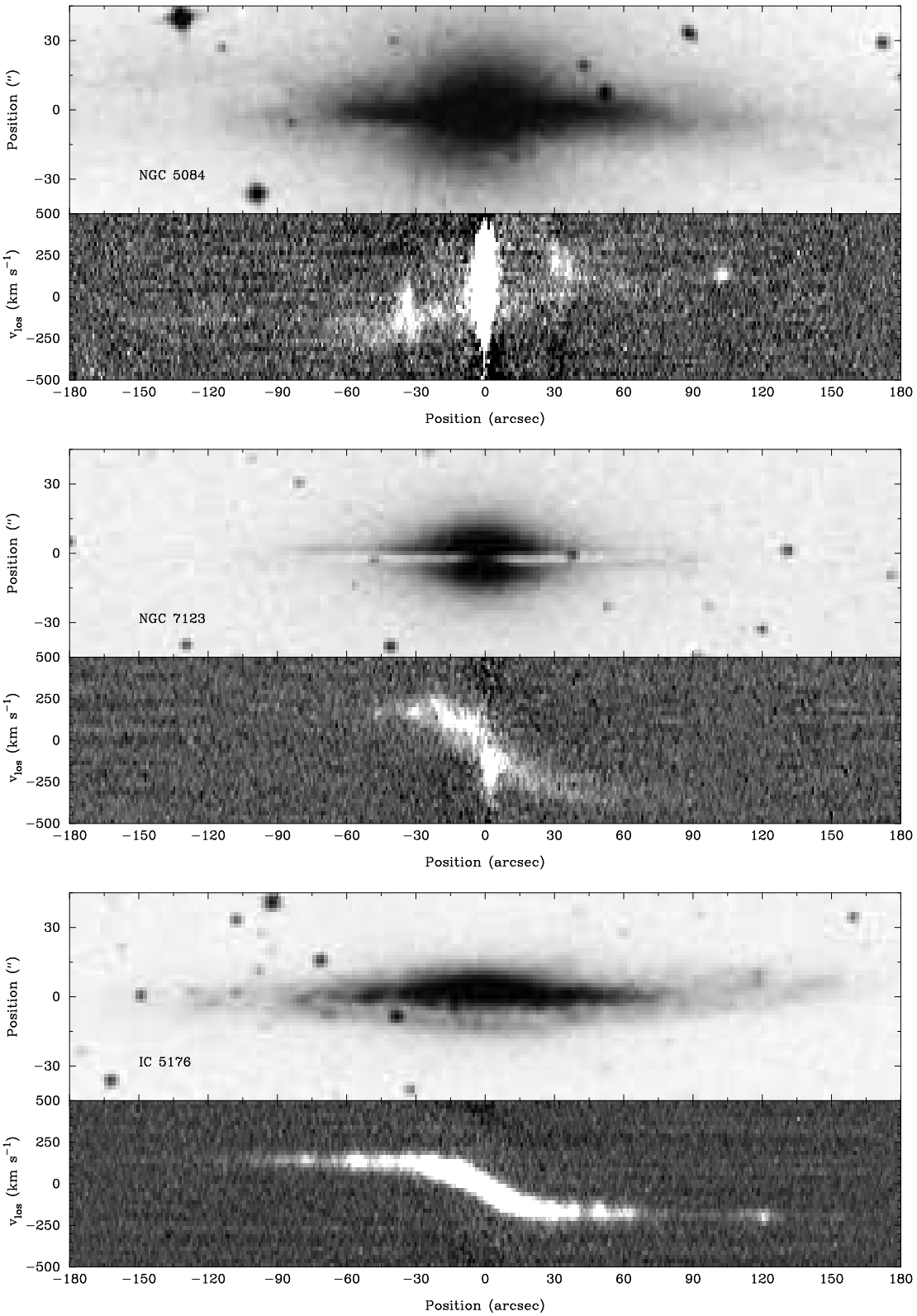

Figure 5.2: *Continued.*

recently and possibly accreted material. These results are tabulated in Table 5.2.

5.5 Discussion

The only previous study of this kind was that of Kuijken & Merrifield (1995), who proposed the method and considered two galaxies. This is thus the first systematic observational study of the relationship between bars and B/PS bulges in spiral galaxies. In summary, our main result is that 14 galaxies out of the 17 galaxies with a B/PS bulge are barred, and the remaining 3 galaxies show evidence of interaction or may be axisymmetric. None of the 6 galaxies in the control sample shows any evidence for a bar.

This means that most B/PS bulges are due to the presence of a thick bar viewed edge-on, and only a few examples may be due to the accretion of external material. In addition, the more spheroidal bulges (i.e. non-B/PS) seem to be axisymmetric. It appears then that most B/PS bulges are edge-on bars, and that most bars are B/PS when viewed edge-on. However, the small size of the control sample prevents us from making a stronger statement about this converse.

If bars were unrelated to the structure of bulges, we would have expected only about 5 galaxies in the main sample to be strongly barred, and about 2 galaxies in the control sample (about 30% of spirals are strongly barred; see Sellwood & Wilkinson 1993). Clearly, our results are incompatible with these expectations.

Our association of bars and B/PS bulges supports the bar-buckling mechanism for the formation of the latter. However, we do not test directly for buckling, but rather for the presence of a barred potential in the plane of the disks. Because bars form rapidly and buckle soon after, on a timescale of only a few dynamical times (see, e.g., Combes et al. 1990), it is unlikely that any galaxy in this nearby sample would have been caught in the act of buckling. Thus, other mechanisms which may lead to thick bars cannot be excluded. In addition, we have no way of determining how the bars themselves formed, or even whether they formed spontaneously in isolation or through interaction with nearby galaxies. Therefore, the possibility of hybrid scenarios for the formation of B/PS bulges, where a bar is formed through an interaction and subsequently thickens due to the buckling instability (see § 5.2.2), remains.

We have looked mainly at objects with large bulges; only two of the galaxies studied are late-type spirals (ESO 240- G 011 and IC 5176). This is a selection effect due to the difficulty of identifying a very small bulge as B/PS. It would therefore be interesting to search for bars in very late-type edge-on spiral galaxies, and verify whether thin bars do exist. The bar in ESO 240- G 011 is not very thick, but it is thicker (isophotally) than the disk. H I synthesis imaging is probably the

best way to achieve this goal, as these objects are often dusty and H I-rich. We will report on H I synthesis observations of a few objects in our sample in a later paper.

In Chapters 3 and 4, we proposed diagnostics, again based on the structure of an observed PVD, to determine the viewing angle with respect to the bar in an edge-on barred disk (see also § 5.3). When the bar is seen close to side-on, the nuclear spiral signature is compact and steep, and the maximum radial velocity it reaches is similar to or larger than the flat portion of the rotation curve. When the bar is seen close to end-on, the nuclear spiral signature extends to relatively large distances and only reaches low velocities. These diagnostics are ideally suited to test the prediction of N-body models, that bars are peanut-shaped when seen side-on and boxy-shaped when seen end-on (see, e.g., Combes & Sanders 1981; Raha et al. 1991).

Of the 12 barred galaxies in the main sample where it is possible to apply these criteria (we exclude NGC 128 and IC 2531), two-thirds (8/12) seem to be consistent with the above prediction from N-body simulations. For example, in the galaxy with a peanut-shaped bulge IC 4937, it is clear that the steep inner component associated with the nuclear spiral extends to higher radial velocities than the outer parts of the disk (see Fig. 5.1). This situation is reversed in NGC 1886, which has a boxy-shaped bulge. However, caution is required when interpreting this result. Firstly, the present classification of the shape of the bulges is affected both by dust and the low dynamic range of the survey material used (Digitized Sky Survey). To remedy this problem, we have acquired K-band images of all the sample galaxies and we will report on these observations in a future paper. Secondly, no clear prediction has been made from N-body simulations about the viewing angle where the transition from a boxy to a peanut-shaped bulge occurs. In that regard, it would be useful to apply quantitative measurements of the boxiness and "peanutness" of the bulges to both observational data and simulation results (see, e.g., Bender & Möllenhoff 1987 and Athanassoula et al. 1990 for two possible methods). Thirdly, because the nuclear spiral is located near the center of the galaxies, the velocities it reaches depend somewhat on the central concentration of the objects (which affects the circular velocity in the central regions). This obviously varies amongst the galaxies in our sample. Therefore, while our observations weakly support the prediction of N-body models concerning the orientation of the bars in B/PS bulges, we believe that it is premature to make a detailed quantitative comparison of the data with the models.

For a more detailed comparison with theory, data of higher signal-to-noise and higher spatial resolution than the average PVD presented here would be very desirable. In that spirit, it would be worthwhile to model individually the best PVDs obtained in the present study (e.g. NGC 5746, IC 5096, and a few others).

This would very likely lead to tight constraints on the mass distribution of the galaxies and the properties of the bar, including the pattern speed (see Ch. 3 and 4).

Because many galaxies in our sample have a prominent dust lane, it is important to consider the possible effects of dust on our observations. The major effect of dust in an edge-on system is to limit the depth to which the line-of-sight penetrates the disk. However, we selected many galaxies to be slightly inclined, so it was possible in those objects to position the slit just above the dust lane, and have a line-of-sight that still goes through most of the disk, as required for a comparison with the models of Chapters 3 and 4. In the few cases with a strong dust lane and a perfectly edge-on disk, we tried again to put the slit just above the dust layer. Unfortunately, with the observational set-up available at the telescope, it was difficult to locate the slit with great precision. The objects where we suspected that dust could affect our observations are indicated in Tables 5.1–5.3.

A large dust optical depth in an edge-on disk produces an almost featureless PVD, and the rotation curve appears slowly-rising and solid-body, as one sees only an outer annulus of material in the disk (see, e.g., Bosma et al. 1992). The only objects showing obvious signs of absorption are IC 2531[3] and NGC 4703 (and possibly ESO 443- G 042). Because we see a lot of structure in most PVDs, including the PVDs of objects with a significant dust lane, we do not believe that our results are significantly affected by dust; we do detect a clear bar signature in most objects of the main sample.

This statement is strengthened by the fact that all the PVDs showing a bar signature are close to symmetric. We showed in Chapter 4 that the bar signature would be strongly asymmetric for a very dusty disk, and this is not observed. Similarly, it is improbable that irregular dust distributions would lead to such well-ordered and symmetric PVDs (very large dust patches would be required to create the gaps observed in many objects).

An unexpected but interesting prospect raised by our observations concerns emission line ratios. For many of the barred galaxies in the main sample, the emission line ratios in the central regions are different from those expected of typical H II regions. For 9 barred galaxies out of 14, mostly those with the strongest bar signatures, the [N II] λ6584 to Hα λ6563 ratio is greater than unity in the bulge region. Furthermore, in a few objects, the steep inner component of the PVD, associated with the nuclear spiral, is much stronger in [N II] than it is in Hα, while the slowly rising component, associated with the outer parts of the disk, has a [N II]/Hα ratio typical of H II regions. In fact, the inner component can be almost absent in Hα. We illustrate those two behaviours in Figure 5.3

[3]This is confirmed by the H I radio synthesis data of Bureau & Freeman (1997), which reveal a complex PVD with a bar signature.

with the PVDs of NGC 5746 and IC 5096.

It is possible that the Hα emission line is weakened by the underlying stellar absorption line. This suggestion is supported by the fact that the spectra of many galaxies show strong Balmer absorption lines. However, the Hα absorption would need to be very large to account for the extreme [N II]/Hα ratios observed in some objects (see, e.g., Fig. 5.3). The strong Balmer lines observed in many objects are interesting in themselves, and indicate that a significant intermediate age ($\sim$ 1 Gyr) stellar population is present in the central regions of the disk of many objects. It would be interesting to see if these past bursts of star formation are related to the presence of the bars.

The high emission line ratios are interesting for two reasons. Firstly, high [N II]/Hα ratios are believed to be produced by shocks (see, e.g., Binette, Dopita, & Tuohy 1985; Dopita & Sutherland 1996). This is consistent with the view that B/PS bulges are simply bars viewed edge-on. The steep inner components of the PVDs, which display high [N II]/Hα ratios, are associated with the nuclear spirals observed in many barred spiral galaxies (see Ch. 4). Athanassoula (1992) showed convincingly that these are the locus of shocks. Secondly, if one were to derive Hα and [N II] rotation curves from the data, by taking the upper envelope of the PVDs (as is usually done), the Hα and [N II] rotation curves would differ significantly for many objects. The Hα line would yield slowly rising rotation curves flattening out at relatively large radii, while the [N II] line would yield rapidly rising rotation curves flattening out at small radii. The mass models derived from such data would thus yield qualitatively different results, and our understanding of galactic dynamics and structure gained from this type of work could be seriously erroneous (at least for highly inclined spirals). Of course, now that we have established that these galaxies are barred, their rotation curves should not be used directly for mass modelling, as they are not a good representation of the circular velocity.

On the other hand, data such as those presented in Figure 5.3 open up the possibility of determining the ionisation conditions and abundance of the gas in different regions of the galaxies. Because the deprojected location of each component of the PVDs is known (see Ch. 4), we can study the effects of bars on the interstellar medium of the galaxies on various scales. A study of this type will be presented in the future.

5.6 Conclusions

In this chapter, we discussed the various mechanisms proposed for the formation of boxy and peanut-shaped bulges in edge-on spiral galaxies. We argued that accretion scenarios were unlikely to account for most boxy/peanut-shaped (B/PS) bulges, but that bar-buckling scenarios, discovered through N-body simulations,

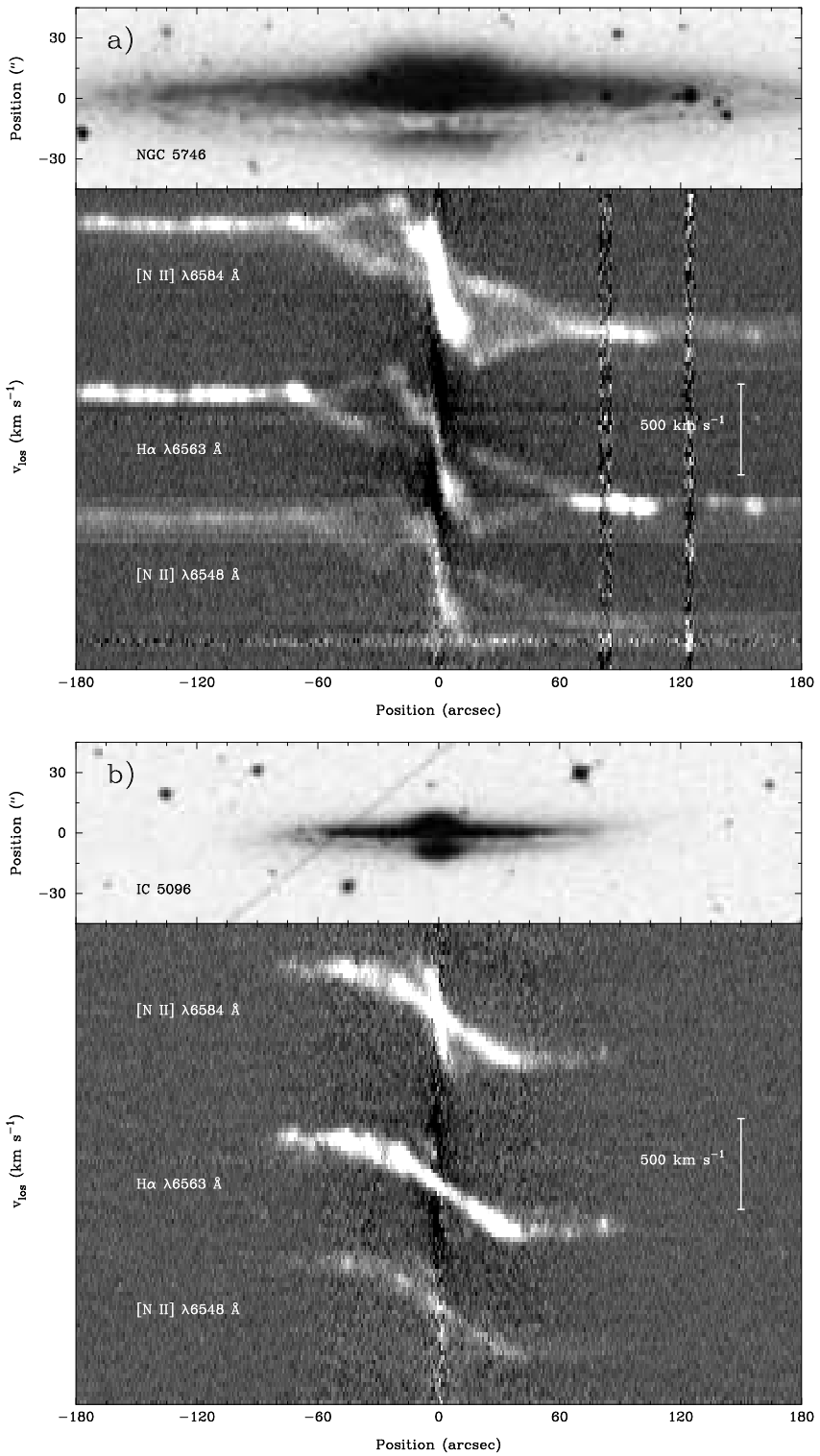

Figure 5.3: Structure and kinematics of (a) NGC 5746 and (b) IC 5096. For each plot, the top panel shows a blue image of the galaxy (Digitized Sky Survey). The bottom panel shows ionised gas position-velocity diagrams (PVDs) of the galaxy along its major axis, registered with the image above it. The PVDs correspond to the [N II] λ6584, Hα λ6563, and [N II] λ6548 emission lines (from top to bottom). Note the large [N II] λ6584 to Hα ratio in the central component of the PVDs.

had this potential. Using kinematical bar diagnostics recently developed for edge-on spirals, we searched for bars in a large sample of edge-on spiral galaxies with a B/PS bulge. Of the 17 galaxies where the diagnostics could be applied using emission lines, 14 galaxies showed the presence of a bar, 2 galaxies were significantly affected by interactions, and 1 galaxy may be axisymmetric. In a control sample of 6 galaxies with a spheroidal bulge, none appeared to be barred.

Our study supports the bar-buckling mechanism for the formation of B/PS bulges. Our results imply that most B/PS bulges are due to the presence of a thick bar viewed edge-on, while only a few may be due to the accretion of external material. Furthermore, spheroidal bulges do appear to be axisymmetric. This suggests that all bars are B/PS. Our observations also seem to support the prediction of N-body simulations, that bars appear boxy-shaped when seen end-on and peanut-shaped when seen side-on. However, this issue should be revisited in a more quantitative manner in the future. With our data, we have no way of determining whether the bars leading to B/PS bulges have formed in isolation or through interactions and mergers. The association of B/PS bulges and bars is entirely consistent with the properties of the bulge of the Milky Way, which is known to be both boxy and bar-like.

We considered the effects of dust on our observations but concluded that it does not affect our results significantly. We have also shown that emission line ratios correlate with kinematical structures in many barred galaxies. This make possible a direct study of the large scale effects of bars on the interstellar medium in disks.

Our study opens up the possibility of studying the vertical structure of bars. Observationally, this has not been done before and represents an interesting spin-off from the use of bar diagnostics in edge-on spiral galaxies. We have obtained K-band images for all our sample galaxies to study their vertical structure and avoid dust-related problems. We will report on their vertical light distribution in a future paper.

References

Araki, S. 1985, Ph.D. Thesis, Massachusetts Institute of Technology

Athanassoula, E. 1992, MNRAS, 259, 345

Athanassoula, E., Morin, S., Wozniak, H., Puy, D., Pierce, M. J., Lombard, J., & Bosma, A. 1990, MNRAS, 245, 130

Athanassoula, E., & Sellwood, J. A. 1986, MNRAS, 221, 213

Bender, R., & Möllenhoff, C. 1987, A&A, 177, 71

Bettoni, D., & Galletta, G. 1994, A&A, 281, 1

Binette, L., Dopita, M. A., & Tuohy, I. R. 1985, ApJ, 297, 476

Binney, J. J., Gerhard, O. E., Stark, A. A., Bally, J., & Uchida, K. I. 1991, MNRAS, 252, 210

Binney, J., & Petrou, M. 1985, MNRAS, 214 449

Bosma, A., Byun, Y., Freeman, K. C., & Athanassoula, E. 1992, ApJ, 400, L21

Bureau, M., & Freeman, K. C. 1997, PASA, 14, 146

Combes, F., Debbasch, F., Friedli, D., & Pfenniger, D. 1990, A&A, 233, 82

Combes, F., & Sanders, R. H. 1981, A&A, 96, 164

Debattista, V. P., & Sellwood, J. A. 1998, ApJ, 493, L5

de Carvalho, R. R., & da Costa, L. N. 1987, A&A, 171, 66

de Souza, R. E., & dos Anjos, S. 1987, A&AS, 70, 465

Dopita, M. A., & Sutherland, R. S. 1996, ApJS, 102, 161

Emsellem, E., & Arsenault, R. 1997, A&A, 318, L39

Fridman, A. M., & Polyachenko, V. L. 1984, Physics of Gravitating Systems (New York: Springer-Verlag)

Friedli, D., & Benz, W. 1993, A&A, 268, 65

Gerin, M., Combes, F., & Athanassoula, E. 1990, A&A, 230, 37

Hamabe, M., & Wakamatsu, K. 1989, ApJ, 339, 783

Hasan, H., & Norman, C. 1990, ApJ, 361, 69

Hernquist, L., & Quinn, P. J. 1989, ApJ, 342, 1

Jarvis, B. J. 1986, AJ, 91, 65

Kalnajs, A. J. 1971, ApJ, 166, 275

———. 1977, ApJ, 212, 637

Karachentsev, I. D., Karachentseva, V. E., & Parnovsky, S. L. 1993, Astron. Nachr., 314, 97

Karachentsev, I. D., Karachentseva, V. E., Parnovsky, S. L., & Kudrya, Y. N. 1993, Astron. & Astrophys. Trans., 4, 143

Kormendy, J., & Illingworth, G. 1982, ApJ, 256, 460

Kuijken, K. 1996, in Barred Galaxies, ed. R. Buta, D. A. Crocker, and B. G. Elmegreen (ASP: San Francisco), 505

Kuijken, K., & Merrifield, M. R. 1995, ApJ, 443, L13

May, A., van Albada, T. S., & Norman, C. A. 1985, MNRAS, 214 131

Merrifield, M. R. 1996, in Barred Galaxies, ed. R. Buta, D. A. Crocker, and B. G. Elmegreen (ASP: San Francisco), 179

Mihos, J. C., Walker, I. R., Hernquist, L., de Oliveira, M. C., & Bolte, M. 1995, ApJ, 447, L87

Miwa, T., & Noguchi, M. 1998, ApJ, 499, 149

Mulder, W. A., & Liem, B. T. 1986, A&A, 157, 148

Noguchi, M. 1987, MNRAS, 228, 635

Norman, C. A., Sellwood, J. A., & Hasan, H. 1996, ApJ, 462, 114

Paczyński, B., Stanek, K. Z., Udalski, A., Szymański, M., Kałużny, J., Kubiak, M., Mateo, M., & Krzemiński, W. 1994, ApJ, 435, L113

Peters, W. L. 1975, ApJ, 195, 617

Pfenniger, D. 1984, A&A, 134, 373

Pfenniger, D., & Friedli, D. 1991, A&A, 252, 75

Raha, N., Sellwood, J. A., James, R. A., & Kahn, F. D. 1991, Nature, 352, 411

Rowley, G. 1986, Ph.D. Thesis, The Australian National University

———. 1988, ApJ, 331, 124

Sellwood, J. A. 1980, A&A, 89, 296

——— 1981, A&A, 99, 362

Sellwood, J. A., & Wilkinson, A. 1993, Rep. Prog. Phys., 56, 173

Shaw, M. A. 1987, MNRAS, 229, 691

———. 1993, MNRAS, 261, 718

Toomre, A. 1966, in Geophysical Fluid Dynamics, 1966 Summer Study Program at Woods Hole Oceanographic Institution, ref. no. 66-46, 111

Weiland, J. L., et al. 1994, ApJ, 425, L81

Weinberg, M. D. 1985, MNRAS, 213, 451

Whitmore, B. C., & Bell, M. 1988, ApJ, 324, 741